

Inferring the dynamics of stellar streams via distance gradients

Shoko Jin^{1*} and Nicolas F. Martin²

¹*Astronomisches Rechen-Institut, Zentrum für Astronomie der Universität Heidelberg, Mönchhofstr. 12–14, D-69120, Heidelberg, Germany*

²*Max-Planck-Institut für Astronomie, Königstuhl 17, D-69117, Heidelberg, Germany*

ABSTRACT

We present a simple result in which the distance gradient along a stream can be used to derive the transverse velocity (i.e. proper motion) along it, if the line-of-sight velocity is also known. We show its application to a mock orbit to illustrate its validity and usage. For less extended objects, such as globular clusters and satellite galaxies being tidally disrupted, the same result can be applied in its small-angle approximation. The procedure does not rely on energy or angular momentum conservation and hence does not require a Galactic model in order to deduce the local velocity vector of the stream.

Key words: Galaxy: kinematics and dynamics — methods: analytical

1 INTRODUCTION

In the last few years, our view of the Milky Way’s stellar halo has been altered by the pioneering work of the Sloan Digital Sky Survey (SDSS) and continued analyses of its data; it is now abundantly clear that the outskirts of the Galaxy provide the prime locations in which to search for signs of ongoing accretion events onto our Galaxy, as well as the remnants of such events, more progressed toward their final dissolution into the Milky Way (Belokurov et al. 2006). Current survey data that enable such studies are mainly photometric, while spectroscopic follow-up is often necessary to check, via its kinematics, whether a photometrically selected stellar grouping is truly an association. Many stellar streams originating from either globular clusters or dwarf galaxies have been identified in the Galactic halo through such investigations. The former can be exemplified by the globular cluster Palomar 5 (Odenkirchen et al. 2001, 2003), while the most prominent example of the latter is the Sagittarius stream (Ibata et al. 1994).

Much of the recent attempts to understand the dynamics of these objects, and thus also their ultimate fate, have come from their modelling via numerical simulations that can now foster millions of particles in a study of a single stellar system. These works illustrate how the tidal distortion and subsequently resulting disruption lead to orbits of constituent stars that deviate from that of the bound parental structure (e.g. Ibata et al. 1997; Dehnen et al. 2004; Johnston et al. 2005; Choi et al. 2007; Montuori et al. 2007). Fully live numerical studies also allow for the possibility of studying disrupting systems under the auspices of dynamical friction. Simulations are therefore key to furthering our understanding of these dynamically evolving stellar substructures, with improvements and advancement continually being made on the incorporation of necessary physics in the correct ratios to model better the systems under study.

It is, however, also interesting to reflect on the extent to which simple geometric or analytic arguments can aid in these quests. Previously, we showed that the radial velocity gradient along a stream can be used to derive the transverse velocity (i.e. proper motion) as a function of distance (Jin & Lynden-Bell 2007; see also Binney 2008), which in turn allows for the determination of orbits for these streams. The success of this method relies on the radial velocity gradient being well determined, and Binney showed its successful application to Palomar 5, by recovering its observationally known properties. The procedure presented in this letter is a related and complementary one, applicable when the distance information for stars in a stream is more abundant (or better constrained) than that for radial velocities. In the following sections, we first present a simple result that can be used to calculate the transverse velocity for a given point along a stellar stream, using knowledge of the distance gradient and the radial velocity there. An application to a mock orbit is then used to illustrate its usage. We also provide a simple geometric visualisation of how the same result can be reached for less extended objects, such as dwarf galaxies that are being tidally disrupted.

2 CONSTRAINING TRANSVERSE MOTION THROUGH DISTANCE GRADIENTS

2.1 The method

Let $d\hat{\mathbf{i}}$ be the heliocentric position vector to a particular point on the stream, with unit line-of-sight vector $\hat{\mathbf{i}}$ and heliocentric distance d , so that its line-of-sight velocity, relative to the Galactic Standard of Rest, is given by $v_l = \mathbf{v} \cdot \hat{\mathbf{i}}$. Differentiating the position vector with respect to time, t , and using the chain rule results in the following:

$$\begin{aligned} \mathbf{v} &= \frac{dd}{dt} \hat{\mathbf{i}} + d \frac{d\hat{\mathbf{i}}}{dt} \\ &= \frac{dd}{d\chi} \frac{d\chi}{dt} \hat{\mathbf{i}} + d \frac{d\hat{\mathbf{i}}}{d\chi} \frac{d\chi}{dt} \end{aligned}$$

* e-mail: shoko@ari.uni-heidelberg.de

$$= \frac{v_s}{d} \frac{dd}{d\chi} \hat{\mathbf{l}} + v_s \hat{\mathbf{s}}, \quad (1)$$

where χ is the angle along the stream, measured from some fiducial point, and $\hat{\mathbf{s}}$ is the unit vector along the apparent direction of motion of the stream at $\hat{\mathbf{l}}$, such that $\hat{\mathbf{s}} = d\hat{\mathbf{l}}/d\chi$ and $d\chi/dt = \mathbf{v} \cdot \hat{\mathbf{s}}/d = v_s/d$ from the usual equation for the transverse velocity. One possible method for calculating $\hat{\mathbf{s}}$ is provided by Jin & Lynden-Bell (2008). By noting that the full velocity vector at any point along a stream is given by $\mathbf{v} = v_l \hat{\mathbf{l}} + v_s \hat{\mathbf{s}}$, we obtain the following relation:

$$v_s = dv_l \left(\frac{dd}{d\chi} \right)^{-1}. \quad (2)$$

This result can also be reached by taking the derivative of the position vector with respect to χ , rather than t . We note that equation (5) of Binney (2008) gives the same result, by identifying the time derivative of the angle as v_s/d .

While equation (2) does not require the value of the Galactic potential at the location of interest as an input, it assumes that the stars of the stream, whose distances are used as an ingredient of the method, are part of the same moving group and that the stellar trajectories follow the observed stream. Under this assumption, the method provides a means of calculating the stream's local transverse velocity, thereby allowing the determination of all components of the velocity vector. In an ideal case, one would have both distance and kinematic data on the stars. However, if both distances and line-of-sight velocities are known, then we could just as easily calculate the transverse velocity through a method that relies on the gradient in v_l (Jin & Lynden-Bell 2007). The result presented in this letter is therefore most useful when the distance gradient along a stream is well determined, and for relatively small uncertainties in the stellar distances (e.g. for RR Lyrae or BHB stars), but when one's knowledge of the kinematics is more limited. On the other hand, if no radial velocity information is available for the stars, one can still determine the ratio of the two velocity components. Hence the family of orbits to be derived for the stream need only be a function of v_l .

Given the simple form of equation (2), the error in the derived transverse velocity is calculated very straight-forwardly through the quadrature sum of the fractional errors in the other quantities:

$$\frac{\Delta v_s}{v_s} = \left(\left(\frac{\Delta Q}{Q} \right)^2 + \left(\frac{\Delta d}{d} \right)^2 + \left(\frac{\Delta v_l}{v_l} \right)^2 \right)^{1/2}, \quad (3)$$

where $Q = dd/d\chi$ and Δx gives the magnitude of the error, or uncertainty, in quantity x . This warns us that if any of the quantities are very small, then its fractional error will significantly boost the error for v_s and that, in particular, a small distance gradient will cause the most damage, given its place in the denominator of equation (2).

2.2 Example application

Figure 1 shows the distance evolution along a mock orbit (in grey), generated using the Milky Way model adopted by Paczyński (1990). The exercise here is to use the distance gradient and a single radial velocity to deduce the transverse velocity at a given point on the stream, and then attempt to recover the input orbit. Within this orbit, we place ourselves at a point mid-way along the segment shown in Figure 1, at $\chi = 8.0^\circ$. The distance gradient is calculated by simply fitting a second-order polynomial (also shown in the same figure by the dot-dashed black line) and taking

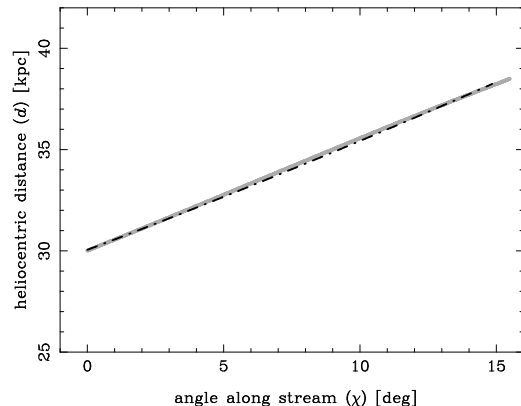


Figure 1. Distance as a function of angle along a small segment of a mock stream (solid grey line), overplotted with a fit deduced using a second order polynomial, $d = a + b\chi + c\chi^2$ (dot-dashed black line); the fit shown has $a = 30.1$, $b = 0.509$, $c = 2.86 \times 10^{-3}$. $\chi = 8.0^\circ$ denotes the location where we choose to calculate the distance gradient in order to deduce the transverse velocity, and hence the location for which the initial conditions for the orbit calculation are subsequently defined.

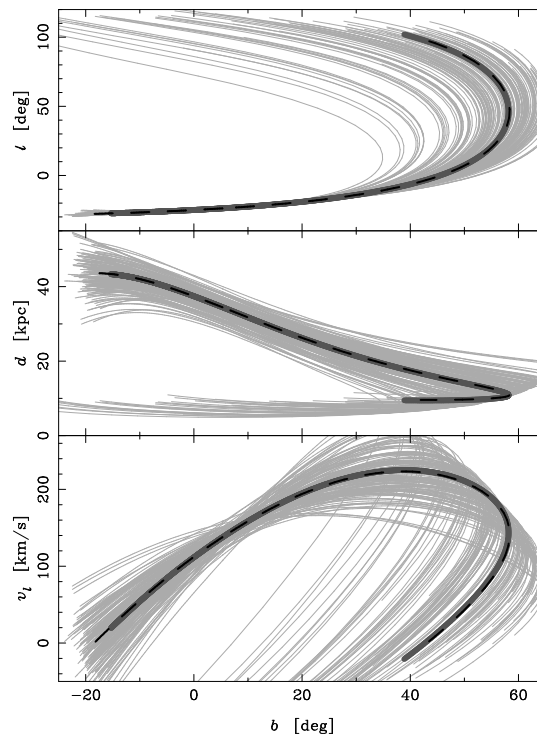


Figure 2. Testing the recovery of the orbital parameters: Galactic longitude (top panel), heliocentric distance (middle panel) and line-of-sight velocities relative to the Galactic Standard of Rest (bottom panel) are shown as functions of Galactic longitude. Original data from the mock orbit are shown in dark grey (solid), whilst those for the recovered orbit are plotted in black (dashed). There are no significant differences between the two orbits over 70° . Also shown in light grey are 147 orbits for which artificial uncertainties were added to the orbital starting point for the distance, line-of-sight velocity and distance gradient; values for each parameter are drawn from a Gaussian distribution centred on the value characterising the correctly recovered orbit, with its 1σ deviation set to 7% that of the distribution mean.

its derivative at the location of interest¹. The heliocentric distance and line-of-sight velocity are 34.5 kpc and 137.9 km s⁻¹, respectively, and through the application of equation (2), we determine the transverse velocity to be 149.4 km s⁻¹. The directional vector \hat{s} is found to be $(-0.014, -0.254, -0.967)$ in Cartesian Galactic coordinates, using equation (16) of Jin & Lynden-Bell (2008) on two locations, separated from the central point by 5°. These allow us to calculate the velocity vector, from which we then have the necessary 6-dimensional phase-space information to derive the orbit. The original orbit is properly recovered in this example, with the Cartesian velocity vector being $(123.5, -93.4, -131.8)$ km s⁻¹ in the deduced orbit at the position specified above, where it was $(123.7, -93.0, -130.8)$ km s⁻¹ in the original orbit. The small deviations in the velocity vector components do not lead to any noticeable difference in any of the orbital parameters over 70°, as shown by the similarity between the solid grey and dashed black lines in Figure 2. Note that $\chi = 8.0^\circ$ in Figure 1 corresponds to a Galactic longitude and latitude of $(\ell, b) = (-23.8, 5.3)^\circ$ in Figure 2.

The panels of Figure 2 also show the results of a simple exercise, whereby the parameters d , v_l and $dd/d\chi$ at the orbital starting point were allowed to vary, in order to mimic and ascertain the possible effects of observational uncertainties for a real stellar stream. Each of the three parameters were drawn from a Gaussian distribution with the mean given by the initial conditions of the correctly recovered orbit, and whose 1σ deviations were set to 7% of the value of the distribution mean. In practice, observational uncertainties are likely to be fractional for distances ($\sim 7\%$ for RR Lyrae and BHB stars) and absolute for velocities (~ 10 km s⁻¹). For the parameters of our mock orbit, 7% of the mean value corresponds to a realistic uncertainty in each of the variables. The resulting set of 147 light grey lines in each of the panels therefore indicate the degree to which the recovered orbit might differ from the original in cases where we might expect the uncertainties for d , v_l and $dd/d\chi$ to each be of the order of a few percent. As expected from this form of artificial ‘degradation’, the agreement of the sky positions is remarkably good within $\pm 20^\circ$ of the orbital starting point, while the distance tends to suffer a constant offset and the recovery of the line-of-sight velocity is not as good. Unsurprisingly, deviations from the original orbit in all orbital parameters become larger with increasing separation from the orbital starting point, with deviations also manifesting themselves strongly near the turning point of the orbit.

It is also necessary to add the usual cautionary note that streams do not follow exact orbits. However, the notion of quantifying their transverse velocity in this way provides a useful tool with which the motions of streams can be studied with limited kinematic information. Figure 2 also highlights that, in general, one should preferentially apply the technique — observations allowing — every $\sim 20^\circ$ along the stream, so as to follow better the stream’s properties and hence determine a realistic orbit.

2.3 Small-angle approximation

The same relation for v_s can be reached in a straight-forward manner in the small-angle regime through simple geometric arguments, when the object of interest is, for instance, a disrupting dwarf

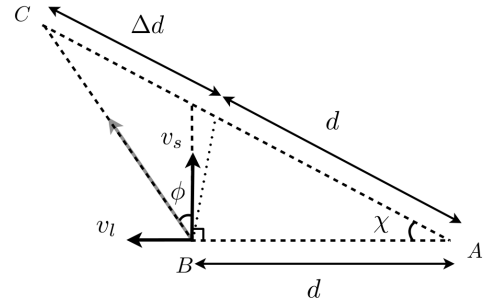


Figure 3. Schematic diagram to illustrate how equation (2) can be reached in the small-angle regime for objects with a more limited angular extent than a generic stellar stream. A denotes the position of the Sun, d is the heliocentric distance to the object at B , and BC gives the true extent of the object with the object’s elongation being along the grey arrow. The difference in distance between the extreme ends of the object is given by Δd , where $\Delta d \ll d$. Equation (2) is recovered straight-forwardly when $\chi \ll 1 \ll \phi$ and the observed elongation of an object is assumed to be a simple projection of its true elongation onto the plane of the sky, with the orbit following the direction of elongation, such that $\tan \phi = v_l/v_s$.

galaxy becoming unbound and is thus no longer self-gravitating. Such a system would exhibit a large elongation and a radial velocity gradient along its extent. In these cases, one assumes that the observed elongation can be de-projected to give the true orbital direction, whose angular difference to the sky projection, ϕ , is given by the relation $\tan \phi = v_l/v_s$. This implies that if the transverse velocity can be estimated through other means, then the variation in distance across the face of the galaxy can be easily deduced (Martin & Jin 2009). Figure 3 illustrates how equation (2) may be reached in such cases, with the pictorial representation showing various quantities in the plane of the orbit. Note that this figure is *not* to scale as, in reality, $\Delta d/d \ll 1$. In cases where χ is small (or, more specifically, when $\chi \ll 1 \ll \phi$), equation (2) is recovered by applying the small-angle approximation directly to Figure 3 and assuming that the true elongation (in the direction of the grey arrow) follows the velocity vector. We also outline below the steps taken to reach the same answer when leaving the application of the approximation to the end; in this case, one can initially employ the sine and cosine rules to obtain exact relations between the various lengths and angles involved.

Let L be the true extent of the object, denoted by BC in Figure 3. Then:

$$\frac{d}{\cos(\phi + \chi)} = \frac{L}{\sin \chi}, \quad (4)$$

$$(d + \Delta d)^2 = d^2 + L^2 + 2dL \sin \phi \quad (5)$$

and

$$d^2 = (d + \Delta d)^2 + L^2 - 2(d + \Delta d)L \sin(\phi + \chi). \quad (6)$$

By taking the difference between equations (5) and (6), and then using (4) to eliminate L , one arrives at equation (2) in the limit that $\chi \ll 1 \ll \phi$ and $\Delta d \ll d$. The latter assumption is only necessary in so far as the fact that the assumed linear elongation, L , should be a good representation of the direction of orbital motion at that location.

¹ The choice of location is reasonably random, apart from avoiding regions with little distance variation; this would lead to unreliable values for v_s as explained in the main text.

3 SUMMARY

This letter presents a simple result that enables the calculation of the transverse velocity along a stream by using the gradient in distance along it. If at least one radial velocity measurement is available and the distance gradient there is known, the transverse velocity at this location can be calculated without the knowledge of the Galactic potential. In these cases, one then has all of the 6-dimensional phase-space information necessary to derive the orbit for the stream. For cases where the radial velocity is not known, one still gains knowledge of the ratio between the radial and transverse velocity components. It is therefore still possible to deduce families of orbits that are functions of the initial radial velocity alone. This result is particularly useful for the study of Galactic stellar streams, in cases where there is a lack of spectroscopic information, but when ample photometric data are available for stellar populations with reliable distance measurements and with small associated errors. With current and future large-sky photometric surveys — such as the SDSS and Pan-STARRS — having the potential to find a multitude of stellar streams in the Milky Way’s halo, we hope that the result presented here will also be useful as a first step in the numerical studies of disrupting stellar substructures in the Galaxy.

Acknowledgements

We thank James Binney and Martin Smith for providing comments on a draft version of this paper. We also thank the referee, Paolo Miocchi, for helpful comments. SJ would also like to thank Eric Bell for discussions which inspired this work.

REFERENCES

- Belokurov V., Zucker D. B., Evans N. W., Gilmore G., Vidrih S., Bramich D. M., Newberg H. J., Wyse R. F. G., Irwin M. J., Fellhauer M., Hewett P. C., et al. 2006, *ApJ*, 642, L137
 Binney J., 2008, *MNRAS*, 386, L47
 Choi J.-H., Weinberg M. D., Katz N., 2007, *MNRAS*, 381, 987
 Dehnen W., Odenkirchen M., Grebel E. K., Rix H.-W., 2004, *AJ*, 127, 2753
 Ibata R. A., Gilmore G., Irwin M. J., 1994, *Nature*, 370, 194
 Ibata R. A., Wyse R. F. G., Gilmore G., Irwin M. J., Suntzeff N. B., 1997, *AJ*, 113, 634
 Jin S., Lynden-Bell D., 2007, *MNRAS*, 378, L64
 Jin S., Lynden-Bell D., 2008, *MNRAS*, 383, 1686
 Johnston K. V., Law D. R., Majewski S. R., 2005, *ApJ*, 619, 800
 Martin N. F., Jin S., 2009, *ApJ*, submitted
 Montuori M., Capuzzo-Dolcetta R., Di Matteo P., Lepinette A., Miocchi P., 2007, *ApJ*, 659, 1212
 Odenkirchen M., Grebel E. K., Dehnen W., Rix H.-W., Yanny B., Newberg H. J., Rockosi C. M., Martínez-Delgado D., Brinkmann J., Pier J. R., 2003, *AJ*, 126, 2385
 Odenkirchen M., Grebel E. K., Rockosi C. M., Dehnen W., Ibata R., Rix H.-W., Stolte A., Wolf C., et al. 2001, *ApJ*, 548, L165
 Paczyński B., 1990, *ApJ*, 348, 485